Radio Frequency From Optical With Instabilities Below 10^{-15}-Generation and Measurement

ARCHITA HATI[1] **(Member, IEEE), MARCO POMPONIO**[1,2]**, NICHOLAS V. NARDELLI**[1]**,**
TANNER GROGAN[1,3]**, KYUNGTAE KIM**[1,3,4]**, DAHYEON LEE**[1,3,4]**, JUN YE**[1,3,4]**,**
TARA M. FORTIER[1]**, ANDREW LUDLOW**[1,2,3]**, AND CRAIG W. NELSON**[1] **(Member, IEEE)**

[1]National Institute of Standards and Technology, Boulder, CO 80305 USA
[2]Department of Electrical, Computer and Energy Engineering, University of Colorado Boulder, Boulder, CO 80309 USA
[3]Department of Physics, University of Colorado Boulder, Boulder, CO 80309 USA
[4]JILA, University of Colorado Boulder, Boulder, CO 80309 USA
CORRESPONDING AUTHOR: A. HATI (archita.hati@nist.gov)

ABSTRACT   This paper presents a frequency synthesis that achieves exceptional stability by transferring optical signals to the radio frequency (RF) domain at 100 MHz. We describe and characterize two synthesis chains composed of a cryogenic silicon cavity-stabilized laser at 1542 nm and an ultra-low expansion (ULE) glass cavity at 1157 nm, both converted to 10 GHz signals via Ti:Sapphire and Er/Yb:glass optical frequency combs (OFCs). The 10 GHz microwave outputs are further divided down to 100 MHz using a commercial microwave prescaler, which exhibits a residual frequency instability of $\sigma_y(1\,\text{s}) < 10^{-15}$ and low 10^{-18} level at a few thousand seconds. Measurements are performed using a newly developed custom ultra-low-noise digital measurement system and are compared to the carrier-suppression technique. The new system enables high-sensitivity evaluation across the entire synthesis chain, from the optical and microwave heterodynes as well as the direct RF signals. Results show an absolute instability of $\sigma_y(1\,\text{s}) \approx 4.7 \times 10^{-16}$ at 100 MHz. This represents the first demonstration of such low instability at 100 MHz, corresponding to a phase noise of -140 dBc/Hz at a 1 Hz offset and significantly surpassing earlier systems. These advancements open new opportunities for precision metrology and timing systems.

INDEX TERMS   Allan deviation, digital measurement system, frequency instability, phase noise, prescalers, optical clocks, optical frequency divider, stability transfer.

I. INTRODUCTION

GENERATING extremely stable radio frequency (RF) signals from optical sources is an important capability that benefits high-precision radar, navigation, communication systems, and metrology. Optical clocks and cavity-stabilized lasers currently set the benchmark for frequency stability and accuracy, outperforming conventional microwave standards by two orders of magnitude both in short and long-term fractional frequency instability [1], [2]. However, translating the extraordinary stability of these optical systems to more accessible RF frequencies, such as 10 MHz and 100 MHz, poses unique challenges. Optical clocks operate at frequencies in the hundreds of terahertz and achieve fractional frequency stabilities below 10^{-16} on short integration times. This remarkable precision will underpin the

redefinition of the SI second [3] and extend the application of optical systems beyond their intrinsic domain. The optical frequency comb (OFC) is central to this effort because it enables phase-coherent division of optical frequencies into the RF and microwave regimes with an exceptional level of spectral purity and stability [4], [5], [6]. While previous developments have mainly focused on generating 10 GHz signals [7], there remains a demand for equally stable signals at lower frequencies, such as 10 MHz and 100 MHz, for applications requiring long-term temporal coherence, and high spectral purity. Currently, 10 MHz signals are widely used as a standard reference frequency in many electronic devices and test instruments, serving as the stable timing source for precise measurements. Additionally, distributing signals at 10 MHz and 100 MHz via coaxial cables is more

convenient due to their low loss compared to microwave signals. Nonetheless, transferring stability from optical to RF regimes is limited by noise in photodiodes, quantum noise, thermal effects, and subsequent frequency divider noise.

This paper demonstrates a system that transfers cavity-stabilized laser stability to 100 MHz and 10 MHz signals with short-term instability levels below 10^{-15} and 10^{-14} respectively. This system will be capable of transferring optical clock stability to domains that are critical for future scientific and industrial applications [8].

FIGURE 1. Block diagram of the optical-to-RF synthesis chain.

II. DESCRIPTION OF OPTICAL-TO-RADIO FREQUENCY SYNTHESIS

Figure 1 shows the block diagram of the optical-to-RF synthesis scheme. It employs a high-finesse cavity-stabilized laser, an OFC, and a microwave prescaler. We constructed two separate synthesis chains: one based on a cryogenic silicon cavity-stabilized laser at 1542 nm [9]; the other utilized an ultra-low-expansion (ULE) glass cavity at 1157 nm [10]. Each respective cavity output was converted to a 10 GHz signal via Ti:Sapphire and Er/Yb:glass OFCs [5], [11]. The 10 GHz microwave outputs were subsequently divided to 100 MHz with commercial prescalers.

A. CAVITY STABILIZED LASERS

The two cavity-stabilized lasers used in the experiment were originally designed and built to probe ultra-narrow atomic resonances in ^{171}Yb [12] and ^{87}Sr [13] optical lattice clocks. These lasers exhibit coherence times of up to several seconds and ultra-low thermally limited phase noise. To achieve such high performance, the lasers are phase-stabilized to Fabry-Perot cavities via a Pound-Drever-Hall (PDH) lock, whereby the length stability of the cavities is transferred to the frequency and phase of the light.

The 1157 nm laser, used to probe the ^{171}Yb clock, is based on a ULE glass cavity at room temperature with a finesse of 877,000. The light is frequency-doubled to reach the clock transition at 578 nm. The 1542 nm laser used to probe the ^{87}Sr clock is based on single-crystal silicon designed to operate at 124 K with a finesse of 500,000. A frequency comb is used to transfer stability to the Sr clock transition frequency at 698 nm. Both optical reference cavities are protected by several layers of thermal isolation, as well as active and passive vibration isolation. The cavities are operated at a temperature at which the coefficient of thermal expansion is nominally zero.

B. OPTICAL FREQUENCY COMBS

We generated the two ultrastable 10 GHz signals for our synthesizer using two optical frequency combs to divide down the optical references. One comb was based on a Ti:Sapphire mode-locked laser producing pulses at a rate of 1 GHz [5], and the other comb was based on an Er/Yb:glass mode-locked laser with a 500 MHz repetition frequency (f_{rep}) [11]. Both combs were fully stabilized with one comb tooth phase-locked to the optical reference laser, v_{opt}, while simultaneously stabilizing the carrier offset frequency, f_o, detected via a f-to-2f interferometer. This transferred the optical reference stability to the comb mode spacing, $f_{rep} = \frac{(v_{opt} - f_o)}{n}$, where n is an integer on the order of 2×10^5. A photodetector converted the laser pulse train to a microwave signal comb with 1 GHz spacing [14]. A bandpass filter (BPF) then selected the desired harmonic of f_{rep}, either 10 GHz or 1 GHz.

In the absence of added photodetector noise, photonically generated microwave signals permit a reduction in the phase modulation (PM) spectral density noise of the optical reference by $(n/m)^2$ when photodetecting the mth harmonic of the OFC repetition rate. When dividing the 1157 nm (259 THz) and 1542 nm (195 THz) optical reference to 10 GHz, this results in a reduction in phase noise by 88 dB and 86 dB, respectively. The phase noise of 10 GHz and 1 GHz signals, scaled to 100 MHz and 10 MHz, is shown later in Section IV.

C. PRESCALERS

We used commercial digital dividers (Microchip Prescaler: UXN40M7KE), which are specified for input frequencies between 500 MHz and 40 GHz with integer division ratios between 1 and 127 [15]. Digital frequency dividers generally support wideband operation with a compact form factor but tend to exhibit relatively high residual phase modulation (PM) noise. In contrast, analog regenerative frequency dividers (RFD) can outperform digital designs in phase noise, but usually offer narrower operating bandwidths and require careful optimization [16], [17], [18], [19]. The digital divider we employed here proved to have very low residual phase noise at offset frequencies below 1 kHz, and showed an exceptionally high stability at output frequencies of 100 MHz. Depending on the divide ratio, this divider's output duty cycle changes from 33% to 66% [15]. The duty cycle is exactly 50% when the divide ratio is a power of 2. For a division factor of 100, the duty cycle is 36% and thus the prescaler output will contain both even and odd harmonics of the fundamental. A bandpass or a lowpass filter can be used at the output of the prescaler to select the desired signal and reject the higher order harmonics.

III. MEASUREMENT TECHNIQUES
A. RESIDUAL PHASE NOISE AND FREQUENCY STABILITY MEASUREMENTS OF PRESCALERS

In previous work [20], we used these microwave prescalers to generate reference signals for characterizing the instability

of 30 GHz divide-by-2 regenerative dividers. However, the result was limited to a fractional frequency instability of $\sigma_y(1\text{ s}) = 1 \times 10^{-15}$ due to measurement system noise floor, even after several days of averaging. These results implied that the residual instability of these digital prescalers was likely below 10^{-15} at 1 s but remained beyond measurement capability using the available digital measurement systems. We also attempted a conventional analog cross-spectrum PM noise measurement [21] but due to high residual amplitude modulation (AM) noise present in the prescalers (see Section IV), the measurement was affected by AM-to-PM conversion in the phase detectors.
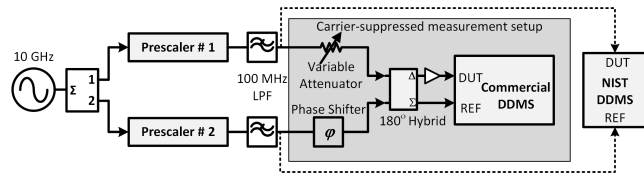

FIGURE 2. Block diagram of the residual measurement schemes used to evaluate a pair of dividers. DDMS: Direct Digital Measurement System.

1) CARRIER-SUPPRESSION TECHNIQUE

To bypass these limitations, we implemented a carrier-suppression (CS) measurement scheme [22], [23], [24] for evaluating a pair of prescalers, as shown in Fig. 2. By summing two phase-aligned signals at the Σ-port and subtracting them at the Δ-port of a 180° hybrid, we increased the effective sensitivity in phase noise measurements proportionally to the amount of carrier suppression achieved. This method is very effective for residual measurements, but it can be challenging for making absolute measurements where a phase locked loop (PLL) is necessary to maintain the phase relationship required for carrier suppression. The frequency response of the PLL suppresses the measurement of longer-term frequency fluctuations, and thus the technique is not ideal for extended averaging of non-residual measurements.

2) DIRECT DIGITAL MEASUREMENT SYSTEM

We used a novel and enhanced performance multichannel direct digital measurement system (DDMS) currently under development at NIST [25], [26]. The DDMS can support up to eight inputs (or channels), however, for this measurement campaign only four inputs were used. By measuring and correcting for aperture jitter, voltage reference and residual flicker noise of the analog-to-digital converters (ADCs), this new DDMS achieves more than a 35 dB reduction in close-to-the-carrier residual phase and amplitude noise, and more than a 20-fold reduction in residual Allan deviation ($\sigma_y(t)$) compared to our previously developed system [27] at 100 MHz carrier. Under ideal conditions, the new DDMS exhibits a single channel residual noise of -147 dBc/Hz at 1 Hz offset, with a flicker-corner of about 30 mHz and a residual frequency stability of 1.3×10^{-16} at a 1 s

averaging time for 100 MHz carriers. Both frequency and time domain performance can be further improved through cross-correlation averaging. For example, with a full-scale input signal of $+9$ dBm at each input, the DDMS 100 MHz noise floor improves to near or below 1×10^{-17} at 1 s for a 0.5 Hz measurement bandwidth [26]. Additionally, the AM-to-PM isolation has been verified to exceed 40 dB at a 1 Hz offset. This capability has enabled unprecedented phase noise and instability measurements of these prescalers at 10 MHz and 100 MHz outputs in both residual and absolute configurations.
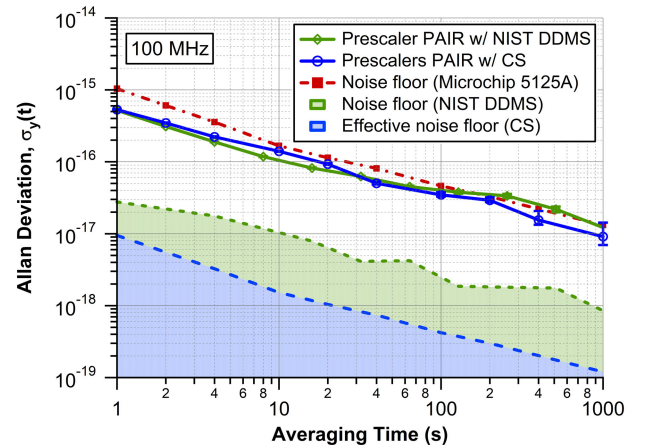

FIGURE 3. Residual fractional frequency instability of a pair of prescalers at 100 MHz measured with the carrier-suppression (CS) and direct digital techniques. Noise floor of carrier-suppression and both commercial and NIST-developed digital measurement systems are also shown. Confidence interval of error bars = 1 sigma, and measurement bandwidth = 0.5 Hz.

We first performed a residual frequency instability comparison of a pair of prescalers, dividing 10 GHz down to 100 MHz, using both the carrier-suppression method and our new digital system. As shown in Fig. 3, the results agreed closely. Unlike the commercial system, the measurement floors of both the carrier-suppression system and the new digital system were sufficiently low to reveal the prescalers' inherent noise. Because the prescalers only provide output power of about $+1$ dBm, the cross-correlated frequency stability floor was slightly degraded, but remained well below 10^{-16} at 1 s. The noise floor of the commercial, CS, and digital measurement systems was measured using a common signal across all channels and at roughly identical power levels as those used for the Allan deviation, absolute, and residual noise measurements.

We also discovered that individual prescalers exhibited up to 6 dB variation in their PM noise, AM noise, and frequency stability performance. To isolate the residual performance of the best prescaler, we used a three-divider approach, also known as the cross-spectrum (or cross-correlation) three-corner hat method [28]. In this configuration, a common signal 'y' generated from the Er/Yb:glass OFC (Fig. 4a)

was used to drive all three prescalers - the device under test (DUT), and two reference prescalers (REF-1 and REF-2) as shown in Fig. 4b. This approach enhances sensitivity of noise measurements by reducing uncorrelated noise from the two reference prescalers by $\sqrt{k}$, where k is the number of FFT averages. This allows an accurate determination of residual phase noise and frequency instability of a single prescaler, the DUT.

B. ABSOLUTE PHASE NOISE AND FREQUENCY STABILITY MEASUREMENTS OF OPTICAL-TO-RF SYNTHESIZERS

We next characterized two optical-to-RF synthesizer chains (Fig. 4a). The cross-spectrum scheme in Fig. 4b measured the absolute phase noise and frequency instability between the two independently generated optical signals, each divided down to 100 MHz. The reference prescalers (REF-1 and REF-2) were connected to a common microwave signal ('y'), while the DUT was driven by the other microwave signal ('x'). This approach measured the combined noise from both cavity-stabilized lasers, both OFCs, their photodiodes, and only one prescaler (the DUT).

Measurements were performed at three points along the synthesis chain. Optical stability was assessed by measuring the heterodyne beat between two cavity-stabilized lasers generated via the Er/Yb:glass frequency comb (output A). Microwave frequency stability was assessed by measuring the heterodyne beat between two 10 GHz signals (output B). Finally, the stability of the 100 MHz prescaler outputs (derived from 10 GHz) was measured directly using a digital system, without heterodyne mixing. A single photodetector and a frequency mixer generated the heterodyne difference frequency for the optical and microwave signals respectively, and the resulting beat signals were also analyzed with the new DDMS. We additionally conducted similar measurements at 10 MHz by dividing the 1 GHz frequency comb signal by 100.

IV. RESULTS

We evaluated the prescalers at two input frequencies and a divide ratio of 100: 10 GHz down to 100 MHz, and 1 GHz down to 10 MHz. Fig. 5 illustrates the absolute phase noise and AM noise at 100 MHz, as well as the phase noise of the optical heterodyne and 10 GHz microwave heterodyne, which are all normalized to 100 MHz. At a 1 Hz offset, the scaled 10 GHz beat had a phase noise of about -153 dBc/Hz which corresponds to -113 dBc/Hz at 10 GHz, while the 100 MHz signals achieved approximately -140 dBc/Hz. For offsets above 0.2 Hz, the phase noise of 100 MHz signal was dominated by the prescaler noise. The prescaler's AM noise was roughly 30 dB higher than its PM noise at 1 Hz offset, which could be problematic with standard analog cross-spectrum techniques due to AM-to-PM conversions at the phase detectors. We initially suspected that the power supply was the source of the relatively high AM noise in the prescalers. To test this, we implemented ultra-low noise
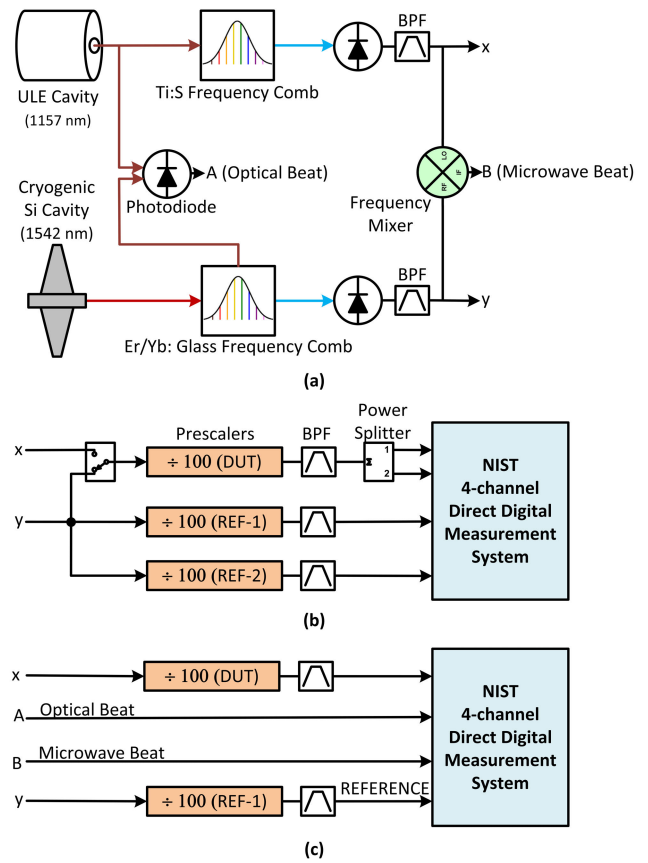

FIGURE 4. Block diagram illustrating measurement of residual noise, absolute noise, and fractional frequency instability of the optical-to-RF synthesis chain. (a) Optical-to-microwave synthesis, and optical beat and microwave beat generation. (b) Microwave-to-RF generation and set-up for residual and absolute noise measurements. For residual measurements, all prescalers were connected to a common signal 'y' and for absolute measurements, the prescaler 'DUT' was connected to 'x' and two reference prescalers were connected to 'y'. A physical switch was not used, it's shown in this block diagram to illustrate the conversion between residual to absolute measurements. (c) Set-up for fractional frequency fluctuations measurement. Signals 'A', 'B', and 'x÷100', were all measured with respect to REFERENCE signal.

voltage regulation. However, this did not alleviate the high level of AM noise, indicating that the source is internal to the prescaler design.

The large spur at 50 kHz frequency offset in Fig. 5 was due to an unintentional heterodyne beat between the two 100 MHz signals that occurred due to insufficient isolation and nonlinearity in the measurement system's input channels.

We also calculated Allan deviation statistics to quantify the frequency instability of the 100 MHz and both heterodyne beats as shown in Fig. 6. The synthesis achieves 4.7×10^{-16} absolute instability at 1 s for the 100 MHz signal. This represents the first demonstration of such low instability at 100 MHz, and significantly surpassing the performance of earlier system [29]. The prescaler alone supported 10^{-18}
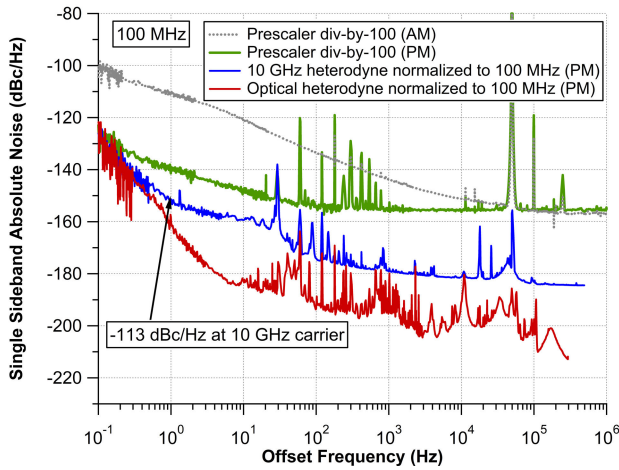
FIGURE 5. Absolute phase noise of optical, microwave (10 GHz) and 100 MHz prescaler output signals. All phase noise plots are normalized to 100 MHz. The AM noise (in gray) is dominated by the prescaler AM noise.
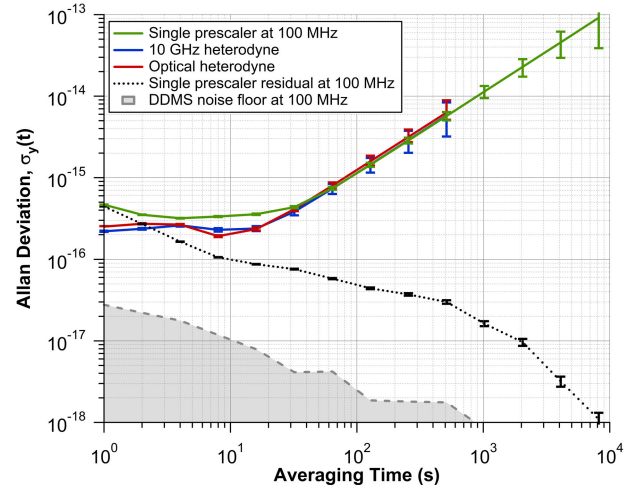

FIGURE 6. Fractional frequency instability of optical, microwave (10 GHz), and 100 MHz signals. It shows the prescaler can transfer the stability of optical signal nearly perfectly without degradation above 20 s. Please note that the single prescaler result is obtained via cross-covariance method. The prescaler demonstrates residual instability of 4.7 x 10^{-16} at 1 s and approaches 10^{-18} at longer averaging time. Confidence interval of error bars = 1 sigma, and measurement bandwidth = 0.5 Hz.

residual stability above 8,000 s when we used the cross-covariance method [28] to remove the reference prescalers' noise. Fig. 7 shows the real-time fractional frequency fluctuations of the optical beat, the microwave beat, and two 100 MHz outputs of a pair prescalers over a 2,000 s interval. These signals clearly show the differential drift between the two cavities. Even if the difference between the optical and the 100 MHz signals showed fluctuations, due to the prescaler residual noise, it remained within the $\pm 4 \times 10^{-15}$ range if the few glitches are ignored. The observed frequency drift was primarily attributed to the ULE cavity, which has a feed-forward drift compensation that was not optimized during these measurements [10], [30]. The configuration depicted in Fig. 4c was used for the evaluation of fluctuations in fractional frequency.

We repeated the above measurements with a microwave heterodyne between two 1 GHz signals (output B), and a direct digital measurement of the 10 MHz prescalers' output (divided down from 1 GHz). The phase noise of the 1 GHz signal does not follow the theoretical noise scaling by n^2 from the optical. As shown in Fig. 8, at a 1 Hz offset, the 1 GHz signal has a phase noise of about -116 dBc/Hz which is only 3 dB lower than the phase noise of 10 GHz signal. This may be due to the photodiode's high flicker noise and/or high relative intensity noise (RIN) of the laser, which can result in excessive phase noise due to AM-to-PM conversion. For the 1 GHz to 10 MHz division, the prescaler's flicker noise contribution was comparatively larger at lower offset frequencies than at 100 MHz output, about -144 dBc/Hz at 1 Hz. The spur around 5 kHz offset was caused by the heterodyne beat between the two 10 MHz input signals. Furthermore, the 10 MHz signal exhibited an absolute fractional instability of $\approx 3 \times 10^{-15}$ at 1 s, for a single prescaler (Fig. 9). Beyond 100 s of averaging, however, the prescaler's impact was negligible, and the absolute instability of the 10 MHz
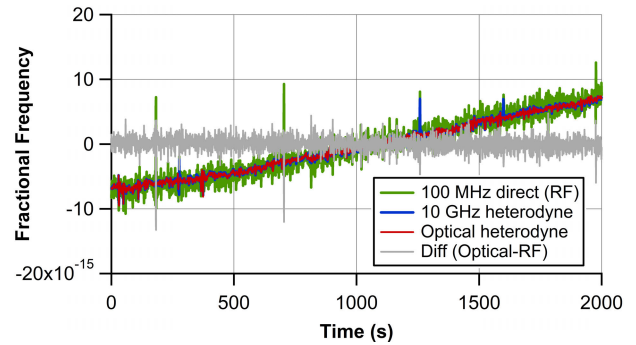

FIGURE 7. Fractional frequency fluctuations between two 100 MHz signals from a pair of prescalers, 10 GHz microwave beat, and optical beat.

signal approached that of the optical reference. The prescaler demonstrates residual instability of $\approx 3 \times 10^{-15}$ at 1 s and approaches 10^{-17} at longer averaging times. The difference of fractional frequency between the optical and the 10 MHz signals showed fluctuations within $\pm 20 \times 10^{-15}$ as shown in Fig. 10.

In addition, multiple prescalers can be used in series for higher division factors. For example, a 1,000 division from 10 GHz to 10 MHz demonstrates a fractional instability of better than 5×10^{-15} at 1 s for two cascaded stages, shown in Fig. 11. In this configuration, the output noise of the first prescaler in the cascade is reduced by n_2^2, where n_2 is the frequency division ratio of the second stage. Therefore, for higher values of n_2, the output noise contribution is dominated by the second stage prescalers.
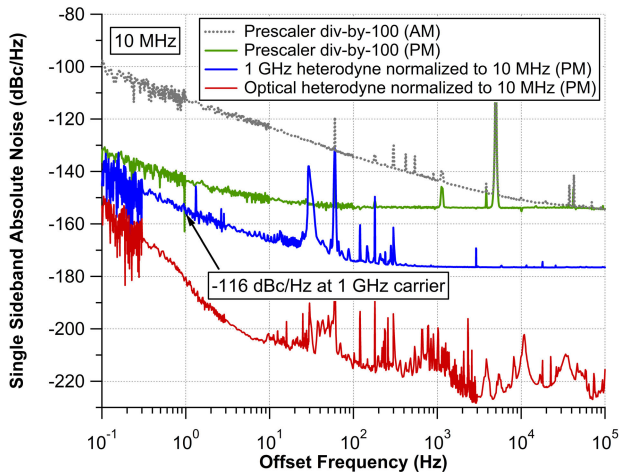
FIGURE 8. Absolute phase noise of optical, microwave (1 GHz) and 10 MHz prescaler output signals. All phase noise plots are normalized to 10 MHz. The AM noise (in gray) is dominated by the prescaler AM noise.
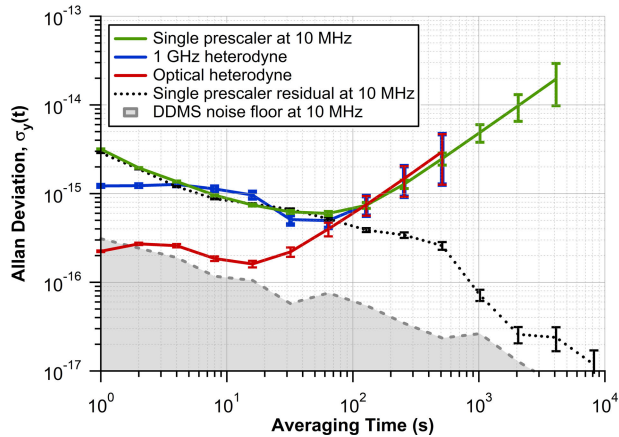

FIGURE 9. Fractional frequency instability of optical, microwave (1 GHz), and 10 MHz signals. It shows the prescaler can transfer the stability of 1 GHz OFC signal nearly perfectly without degradation above 3 s. Please note that the single prescaler result is obtained via the cross-covariance method. The prescaler demonstrates residual instability of $\approx 3 \times 10^{-15}$ at 1 s and approaches 10^{-17} at longer averaging times. Confidence interval of error bars = 1 sigma, and measurement bandwidth = 0.5 Hz.

Frequency instability measurements at this level is highly sensitive to environmental effects. Long-term residual and absolute measurements were performed at night or on weekends to prevent vibration induced disturbances. Although, the microwave-to-RF synthesis sections were sensitive to vibration and temperature, no active stabilization was used other than shielding the prescalers from direct airflow from the heating, ventilation, and air conditioning (HVAC) system. The environmental effect on the long-term measurements was hidden by the drift between the cavities. If these measurements were to be repeated, with the optical cavities locked to their respective atoms, it is likely that environmental stabilization would be needed.
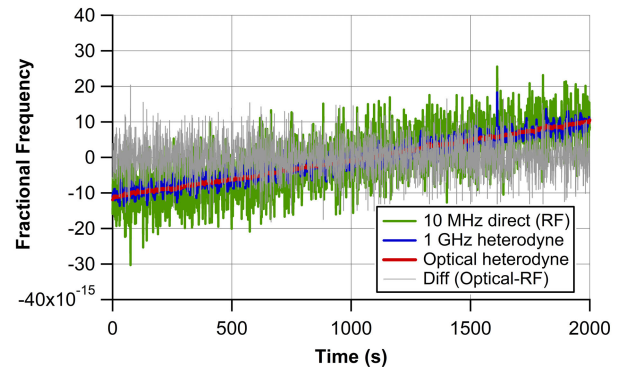

FIGURE 10. Fractional frequency fluctuations between two 10 MHz signals from a pair of prescalers, 1 GHz microwave beat, and optical beat over 2,000 s.
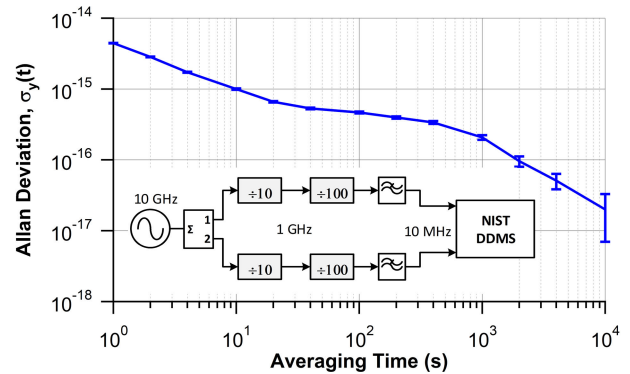

FIGURE 11. Fractional frequency instability of a pair of cascaded prescalers dividing 10 GHz to 10 MHz. Confidence interval of error bars = 1 sigma, and measurement bandwidth = 0.5 Hz.
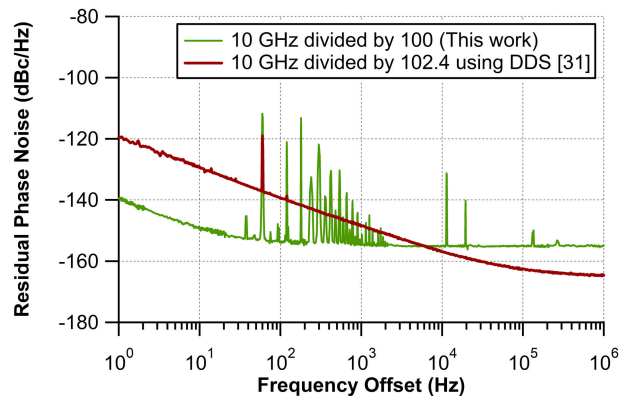

FIGURE 12. Comparison of residual phase noise of digital dividers for a frequency division factor of about 100 for a carrier frequency of 10 GHz.

Finally, Fig. 12 compares the residual noise of this commercial prescaler with that of a typical DDS [31] for a 10 GHz input frequency. For the prescaler and the DDS, respectively, frequency division factors of 100 and 102.4 were selected. The prescaler we employed exhibits phase noise that is almost 20 dB lower than the DDS at a 1 Hz offset. However, the DDS

performs better than the prescaler in the white phase noise region; this discrepancy results from the use of two distinct output driver technologies. A DDS uses an analog output via a digital-to-analog converter, which exhibits a signal-to-noise ratio (SNR) related to quantization noise proportional to the effective number of bits. In contrast, a prescaler's white noise is directly linked to the SNR that comes from the logic states in the digital output driver of the prescaler.

V. CONCLUSION

We presented frequency division from the optical domain down to 100 MHz with an absolute instability of 4.7×10^{-16} at 1 s, corresponding to a phase noise of -140 dBc/Hz at a 1 Hz offset. To our knowledge, this is the first demonstration of 100 MHz signals achieving this level of stability, surpassing previous approaches of optical-to-RF synthesis using regenerative frequency dividers [19], parallel DDS technique [31], microwave frequency synthesizer [32] or generation directly from cryogenic oscillators [33], [34]. We achieved this performance utilizing ultra-high stability commercial frequency prescalers. This is also the first time that 100 MHz measurements, at this level, were performed directly without utilizing a heterodyne beat to increase sensitivity using a newly developed multi-channel digital measurement system with state-of-the-art level performance. This system exhibits a single channel residual noise of -147 dBc/Hz at 1 Hz offset, and a residual frequency stability of 1.3×10^{-16} at a 1 s averaging time for 100 MHz carriers. Additionally, 10 MHz RF signals were generated from the optical domain, and we observed absolute fractional instabilities on the order of $\approx 3 \times 10^{-15}$ at 1 s, dominated by prescaler noise. This study finds that these high performance prescalers can transfer the pristine stability of the optical clocks to usable RF frequencies and will be able to facilitate ultrastable frequency references for future precision metrology and timing systems.

DISCLAIMER

Certain equipment, instruments, software, or materials are identified in this paper to specify the experimental procedure adequately. Such identification is not intended to imply recommendation or endorsement of any product or service by NIST, nor is it intended to imply that the materials or equipment identified are necessarily the best available for the purpose.

REFERENCES

[1] H. Katori, "Optical lattice clocks and quantum metrology," *Nature Photon.*, vol. 5, no. 4, pp. 203–210, Apr. 2011. [Online]. Available: https://www.nature.com/articles/nphoton.2011.45

[2] A. D. Ludlow, M. M. Boyd, J. Ye, E. Peik, and P. O. Schmidt, "Optical atomic clocks," *Rev. Modern Phys.*, vol. 87, no. 2, pp. 637–701, Jun. 2015. [Online]. Available: https://link.aps.org/doi/10.1103/RevModPhys.87.637

[3] N. Dimarcq et al., "Roadmap towards the redefinition of the second," *Metrologia*, vol. 61, no. 1, Jan. 2024, Art. no. 012001, doi: 10.1088/1681-7575/ad17d2.

[4] D. J. Jones et al., "Carrier-envelope phase control of femtosecond mode-locked lasers and direct optical frequency synthesis," *Science*, vol. 288, no. 5466, pp. 635–639, Apr. 2000. [Online]. Available: https://www.science.org/doi/10.1126/science.288.5466.635

[5] T. M. Fortier et al., "Generation of ultrastable microwaves via optical frequency division," *Nature Photon.*, vol. 5, no. 7, pp. 425–429, Jul. 2011. [Online]. Available: https://www.nature.com/articles/nphoton.2011.121

[6] X. Xie et al., "Photonic microwave signals with zeptosecond-level absolute timing noise," *Nature Photon.*, vol. 11, no. 1, pp. 44–47, Jan. 2017. [Online]. Available: https://www.nature.com/articles/nphoton.2016.215

[7] T. Nakamura et al., "Coherent optical clock down-conversion for microwave frequencies with 10^{-18} instability," *Science*, vol. 368, no. 6493, pp. 889–892, May 2020. [Online]. Available: https://www.science.org/doi/10.1126/science.abb2473

[8] J. Yao et al., "Optical-Clock-Based time scale," *Phys. Rev. Appl.*, vol. 12, no. 4, Oct. 2019, Art. no. 044069. [Online]. Available: https://link.aps.org/doi/10.1103/PhysRevApplied.12.044069

[9] D. Matei et al., "1.5 μ M lasers with sub-10 mHz Linewidth," *Phys. Rev. Lett.*, vol. 118, no. 26, Jun. 2017, Art. no. 263202. [Online]. Available: http://link.aps.org/doi/10.1103/PhysRevLett.118.263202

[10] M. Schioppo et al., "Ultrastable optical clock with two cold-atom ensembles," *Nature Photon.*, vol. 11, no. 1, pp. 48–52, Jan. 2017. [Online]. Available: https://www.nature.com/articles/nphoton.2016.231

[11] N. V. Nardelli, H. Leopardi, T. R. Schibli, and T. M. Fortier, "Optical and microwave metrology at the 10^{-18} level with an Er/Yb: Glass frequency comb," *Laser Photon. Rev.*, vol. 17, no. 4, 2023, Art. no. 2200650. [Online]. Available: https://onlinelibrary.wiley.com/doi/pdf/10.1002/lpor.202200650

[12] W. F. McGrew et al., "Atomic clock performance enabling geodesy below the centimetre level," *Nature*, vol. 564, no. 7734, pp. 87–90, Dec. 2018. [Online]. Available: https://www.nature.com/articles/s41586-018-0738-2

[13] A. Aeppli, K. Kim, W. Warfield, M. S. Safronova, and J. Ye, "Clock with 8×10^{-19} systematic uncertainty," *Phys. Rev. Lett.*, vol. 133, no. 2, Jul. 2024, Art. no. 023401. [Online]. Available: https://link.aps.org/doi/10.1103/PhysRevLett.133.023401

[14] Z. Li et al., "High-power high-linearity flip-chip bonded modified uni-traveling carrier photodiode," *Opt. Exp.*, vol. 19, no. 26, pp. B385–B390, Dec. 2011. [Online]. Available: https://opg.optica.org/oe/abstract.cfm?uri=oe-19-26-B385

[15] *UXN40M7K-Prescaler*. Accessed: Jun. 1, 2021. [Online]. Available: https://www.microchip.com/en-us/product/uxn40m7k-prescaler

[16] R. L. Miller, "Fractional-frequency generators utilizing regenerative modulation," *Proc. IRE*, vol. 27, no. 7, pp. 446–457, Jul. 1939.

[17] E. Rubiola, M. Olivier, and J. Groslambert, "Phase noise in the regenerative frequency dividers," *IEEE Trans. Instrum. Meas.*, vol. 41, no. 3, pp. 353–360, Jun. 1992.

[18] A. Gupta, J. F. G. Nava, and F. L. Walls, "A novel low noise regenerative divide-by-four circuit," in *Proc. IEEE Int. Freq. Control Symp. PDA Exhib.*, May 2003, pp. 680–684.

[19] A. Hati, C. W. Nelson, C. Barnes, D. Lirette, J. A. Desalvo, and D. A. Howe, "Ultra-low-noise regenerative frequency divider," *IEEE Trans. Ultrason., Ferroelectr., Freq., Control*, vol. 59, no. 11, pp. 2596–2598, Nov. 2012.

[20] A. Hati, M. Pomponio, C. Humiston, J. Lettang, and C. W. Nelson, "30 GHz regenerative frequency divide-by-3," in *Proc. Joint Conf. Eur. Freq. Time Forum IEEE Int. Freq. Control Symp.*, Apr. 2022, pp. 1–4. [Online]. Available: https://ieeexplore.ieee.org/document/9850942

[21] W. Walls, "Cross-correlation phase noise measurements," in *Proc. 46th. IEEE Freq. Control Symp.*, May 1992, pp. 257–261.

[22] K. H. Sann, "The measurement of near-carrier noise in microwave amplifiers," *IEEE Trans. Microw. Theory Techn.*, vol. MTT-16, no. 9, pp. 761–766, Sep. 1968.

[23] E. N. Ivanov, M. E. Tobar, and R. A. Woode, "Microwave interferometry: Application to precision measurements and noise reduction techniques," *IEEE Trans. Ultrason., Ferroelectr. Freq., Control*, vol. 45, no. 6, pp. 1526–1536, Nov. 1998.

[24] A. Hati, M. Pomponio, and C. W. Nelson, "Ultralow PM and AM noise generation with an ensemble of phase-coherent oscillators," *IEEE Trans. Ultrason., Ferroelectr., Freq., Control*, vol. 71, no. 2, pp. 332–339, Feb. 2024. [Online]. Available: https://ieeexplore.ieee.org/document/10355054

[25] M. Pomponio, "Oscillator measurement system and method with flicker-noise suppression, provisional patent #63/748,774," U.S. Patent 63 748 774, Jan. 23, 2025.

[26] M. Pomponio, A. Hati, and C. Nelson, "Flicker suppressed direct digital: Next generation of measurement systems for time and frequency metrology," *IEEE Trans. Ultrason., Ferroelectr., Freq., Control*, 2025.

[27] M. Pomponio, A. Hati, and C. Nelson, "Direct digital simultaneous phase-amplitude noise and Allan deviation measurement system," *IEEE Open J. Ultrason., Ferroelectr., Freq. Control*, vol. 4, pp. 160–170, 2024. [Online]. Available: https://ieeexplore.ieee.org/document/10737107

[28] D. Fest, J. Groslambert, and J.-J. Gagnepain, "Individual characterization of an oscillator by means of cross-correlation or cross-variance method," *IEEE Trans. Instrum. Meas.*, vol. IM-32, no. 3, pp. 447–450, Sep. 1983.

[29] A. Hati et al., "State-of-the-art RF signal generation from optical frequency division," *IEEE Trans. Ultrason., Ferroelectr., Freq., Control*, vol. 60, no. 9, pp. 1796–1803, Sep. 2013.

[30] W. R. Milner et al., "Demonstration of a timescale based on a stable optical carrier," *Phys. Rev. Lett.*, vol. 123, no. 17, Oct. 2019, Art. no. 173201. [Online]. Available: https://link.aps.org/doi/10.1103/PhysRevLett.123.173201

[31] M. Pomponio, A. Hati, and C. Nelson, "Ultra-low phase noise frequency division with array of direct digital synthesizers," *IEEE Trans. Instrum. Meas.*, vol. 73, pp. 1–10, 2024. [Online]. Available: https://ieeexplore.ieee.org/document/10373048

[32] L.-L. Yan et al., "Photonic generation of RF and microwave signal with relative frequency instability of 10^{-15}," *Chin. Phys. B*, vol. 27, no. 3, Mar. 2018, Art. no. 030601, doi: 10.1088/1674-1056/27/3/030601.

[33] C. E. Calosso, F. Vernotte, V. Giordano, C. Fluhr, B. Dubois, and E. Rubiola, "Frequency stability measurement of cryogenic sapphire oscillators with a multichannel tracking DDS and the two-sample covariance," *IEEE Trans. Ultrason., Ferroelectr., Freq., Control*, vol. 66, no. 3, pp. 616–623, Mar. 2019. [Online]. Available: https://ieeexplore.ieee.org/document/8471219

[34] W. A. Al-Ashwal, A. Hilton, A. N. Luiten, and J. G. Hartnett, "Low phase noise frequency synthesis for ultrastable X-band oscillators," *IEEE Microw. Wireless Compon. Lett.*, vol. 27, no. 4, pp. 392–394, Apr. 2017. [Online]. Available: https://ieeexplore.ieee.org/document/7891948/?arnumber=7891948

ARCHITA HATI (Member, IEEE) is currently an Electronics Engineer with the Time and Frequency Division, National Institute of Standards and Technology, Boulder, CO, USA, where she is the Calibration Service Leader of the Phase Noise Metrology Group. Her research interests include phase noise metrology, ultralow-noise frequency synthesis, the development of low-noise microwave and opto-electronic oscillators, and vibration analysis.

Dr. Hati is a member of the Technical Advisory Committee of the International Union of Radio Science (URSI) Commission A. She is an Elected Administrative Committee (AdCom) Member of IEEE UFFC-S. She was a recipient of the Allen V. Astin Measurement Science Award "For developing a world-leading program of phase noise research and measurement services to support industry and national priorities" in 2015 and the IEEE Cady Award "For groundbreaking contributions to the field of phase noise metrology and advances in the development of ultra-low noise frequency sources and synthesis" in 2024. She served as an Associate Editor for IEEE TRANSACTIONS ON ULTRASONICS, FERROELECTRICS, AND FREQUENCY CONTROL, for three years.

MARCO POMPONIO received the M.Sc. degree in electronic engineering from the Polytechnic University of Turin, Italy, in 2017, in collaboration with Italian National Metrology Institute (INRIM), and the Ph.D. degree from the University of Colorado Boulder in 2025 in collaboration with the National Institute of Standards and Technology (NIST). His research interests include high-performance digital control loops, field programmable gate arrays (FPGA), signal processing, low-noise electronics, and phase and amplitude noise metrology. He won the student poster competition at European Frequency and Time Forum (EFTF) in 2018 and he won the same competition again in 2021 and 2024. He also won the PML Distinguished Associate Award from NIST in 2021.

NICHOLAS V. NARDELLI received the Ph.D. degree from the University of Colorado Boulder in 2023. He worked on the construction of robust and ultra-low noise optical frequency combs at the University of Colorado Boulder, which have enabled the highest stability and accuracy in atomic clock experiments. He is currently a Postdoctoral Researcher at the National Institute of Standards and Technology, Boulder, CO, USA. His current research interests include the application of frequency stabilization techniques to the synchronization and stabilization of single-photon quantum systems.

TANNER GROGAN, photograph and biography not available at the time of publication.

KYUNGTAE KIM was born in South Korea. He received the Ph.D. degree in physics from KAIST, South Korea, in 2021. Since 2021, he has been a Postdoctoral Researcher at JILA, University of Colorado Boulder, USA. He helped set up and studied a quantum gas experiment with lithium atoms at KAIST. His current research interest includes the physics in strontium optical lattice clock experiments.

DAHYEON LEE, photograph and biography not available at the time of publication.

JUN YE, photograph and biography not available at the time of publication.

TARA M. FORTIER, photograph and biography not available at the time of publication.

ANDREW LUDLOW, photograph and biography not available at the time of publication.

CRAIG W. NELSON (Member, IEEE) is currently an Electrical Engineer and the Leader of the Phase Noise Metrology Group at the National Institute of Standards and Technology (NIST), Boulder, CO, USA. He has authored more than 70 articles and teaches classes, tutorials, and workshops at NIST, the IEEE Frequency Control Symposium, and several sponsoring agencies on the practical aspects of high-resolution phase noise metrology. His involvement in this group spans over three decades. His research interests include phase and amplitude noise metrology, low-noise electronics, FPGA-based digital control, and instrument control. He was a recipient of the NIST Bronze Medal in 2012, the Allen V. Astin Measurement Science Award "For developing a world-leading program of phase noise research and measurement services to support industry and national priorities" in 2015, and the IEEE Cady Award "For leadership in the design and development of state-of-the-art low noise oscillators and phase noise measurement systems" in 2020.

• • •